THE JOURNAL OF PHYSICAL CHEMISTRY B

 VOLUME 108, NUMBER 12, MARCH 25, 2004

LETTERS

Calcium and Strontium Hexaluminates: NMR Evidence that "Pentacoordinate" Cation Sites Are Four-Coordinated

Lin-Shu Du and Jonathan F. Stebbins*

Department of Geological and Environmental Sciences, Stanford University, Stanford, California 94305-2115

Received: November 26, 2003

We report new, high-resolution solid state ^{27}Al NMR data for two members of the magnetoplumbite group of structures, strontium hexaluminate ($SrAl_{12}O_{19}$, "SA6") and calcium hexaluminate ($CaAl_{12}O_{19}$, "CA6," synthetic hibonite), acquired at 14.1 and 18.8 T fields. The high-field data allow, for the first time, the accurate observation of the NMR signal from the Al(2) sites, which have been previously described as "pentacoordinate" but which appear instead to be very distorted tetrahedra, which give rise to ^{27}Al isotropic chemical shifts of about 57 ppm and nuclear quadrupolar coupling constants of about 21 MHz. This finding is fully consistent with "split-atom" refinements of these crystal structures, in which the most probable position of the Al atom is displaced away from the average trigonal pyramidal site center, along the crystallographic 3-fold axis. The NMR data also demonstrate, however, that the "splitting" is the result of static, not dynamical, disorder among these sites.

Introduction

Calcium and strontium hexaluminates ($CaAl_{12}O_{19}$, "CA6" and $SrAl_{12}O_{19}$, "SA6") are members of the "magnetoplumbite" group of structures, comprising a diverse set of oxide materials.[1] An intriguing and nearly unique feature of this structure in its ideal ($P6_3/mmc$) space group is a pentacoordinate, trigonal bipyramidal cation site, occupied by Al^{3+} in the aluminates (M2 or Al(2) site[2,3]). In recent structure refinements, it has often been found that a "split atom" model for the "pentacoordinate" site provides a better fit to the diffraction data, with 50% occupancy at positions displaced in opposite directions from the center of the site along the 3-fold axis.[1,4−6] However, it is also generally unclear from diffraction data whether this "splitting" is the result of rapid ion hopping between two potential minima within each individual pentacoordinate site, or whether a model of static disorder is more appropriate. In the latter, each such Al^{3+} would in fact be fixed in a highly distorted tetrahedron.[1]

Because of their unusual structure and the potential utility of CA6 in tough ceramic composites,[7] and because CA6 is the pure, synthetic form of the mineral hibonite,[6] these phases have been widely studied by X-ray diffraction and, more recently, by high-resolution ^{27}Al NMR. The latter has the potential to resolve the issue of static vs dynamic disorder in the "pentacoordinate" site, because observed parameters such as the isotropic chemical shift (δ_{iso}), quadrupolar coupling constant (C_Q), and quadrupolar asymmetry parameter (η) respond to the real, local structure, not the long-range, spatially averaged structure as in diffraction measurements. In particular, δ_{iso} has been considered to be diagnostic of the coordination number of Al by O in oxides, with values (excluding phosphates) of about 85 to 55 ppm indicating four-coordination, values between about 16 and 0 ppm indicating six coordination, and a few known examples of five-coordinated sites lying between with values in the range 50 to 30 ppm.[8,9] CA6 and SA6 have thus been especially interesting in attempts to refine the range for pentacoordinate aluminum to help in the interpretation of spectra for unknown structures such as oxide glasses.[10−12]

* Corresponding author. E-mail: stebbins@pangea.stanford.edu

10.1021/jp037615d CCC: $27.50
Published on Web 03/02/2004

CA6 and SA6 in the ideal magnetoplumbite structure should contain 12/24, 4/24, and 2/24 of the total Al in three distinct octahedral sites, 4/24 in a single tetrahedral site, and 2/24 in the pentacoordinate site.[13] However, NMR characterization of the latter has proven to be difficult. An early study of CA6 done at fields to 11.7 T reported a composite peak in the region expected for the octahedral Al sites, and a single peak for the tetrahedral site, but no obvious signal in the intermediate frequency range expected for AlO_5 groups, perhaps because of unusually large quadrupolar broadening.[13] Much improved spectra obtained at higher fields (to 14.1 T) and higher magic-angle spinning rates still did not reveal the pentacoordinate site and led to further speculation that dynamic site hopping within the trigonal bipyramids could result in disorder, additional peak broadening, and enhanced difficulty of observation.[14] A pioneering study of the ^{27}Al quadrupolar nutation spectra of CA6 suggested that the signal from the pentacoordinate site was overlapped with peaks for the AlO_6 sites and indicated that its apparent C_Q was consistent with a simple point charge calculation based on the average, symmetrical ("unsplit") five-coordinate geometry.[15] A detailed study of SA6 using MAS NMR at fields to 14.1 T, careful analysis of the effects of field on line shapes, and five-quantum MAS again concluded that the AlO_5 signal overlapped extensively with those of the AlO_6 sites and resulted in a fitted model indicating $\delta_{iso} = 18.0$ ppm, $C_Q = 2.1$ MHz, and $\eta = 0.7$ for the former.[16] That study also tabulated δ_{iso} data for pentacoordinate Al sites in oxides and pointed out the anomalously low value of the SA6 result, exceeded only by AlO_5 sites in two aluminum phosphates; possible effects of "split-atom" disordering in broadening of NMR peaks were noted as well. Most recently, a study at fields to 14.1 T of CA6 reached similar conclusions: that the signal from the AlO_5 site was poorly resolved from those of the AlO_6 sites, but could be modeled with a surprisingly low δ_{iso} value of 20 ppm.[17] A value of $\eta = 0$ was retained in the model, consistent with the 3-fold symmetry axis that passes through the site in all crystal structure refinements.

As part of an extensive new high-resolution NMR study of Sr and Ca aluminates, we have collected ^{27}Al high-speed MAS and 3QMAS spectra of CA6 and SA6 at fields of 14.1 and 18.8 T. For the first time, these data reveal the true nature of the "pentacoordinate" sites in these phases, which in fact have static, highly distorted tetrahedral geometries as predicted by a static, "split atom" model.[1] Extremely large C_Q values ($\approx$21 MHz) are apparently responsible for the previous non- or incorrect observations of these sites at lower fields. Observed values of δ_{iso} of about 57 ppm are consistent with such a tetrahedral environment, while our direct observation of zero quadrupolar asymmetry is again consistent with the long-range symmetry.

Synthesis and NMR Experiments

Isotopically normal samples of SA6 and CA6 were prepared from $SrCO_3$ or $CaCO_3$ and dehydrated $Al(OH)_3$, which were ground together in stoichiometric proportions, heated for 5 h at 1500 °C in air, then reground and packed into Pt tubes. These were heated for 14 h at 1500 °C, then were reground and sintered for a final 48 h at the same temperature. Powder XRD showed only the desired hexaluminate phases.

As part of a larger study of ^{27}Al and ^{17}O spectra of Sr aluminates, an ^{17}O-enriched sample of SA6 was also synthesized, necessitating somewhat different methods to ensure retention of the isotopic label. Carefully dried SrO was ground together with 0.2 wt % Co_3O_4 (to speed ^{17}O spin−lattice relaxation) and the stoichiometric amount of $\approx$20% ^{17}O-enriched Al_2O_3, the latter obtained by hydrothermal exchange of $Al(OH)_3$ with labeled H_2O followed by dehydration under Ar. The starting mixture was packed into a Pt tube, which was then welded shut and heated for 8 h at 1420 °C. The sample was then reground, packed into the tube again, and heated for an additional 4 h at the same temperature. Subsequent NMR studies indicated that the relatively small sample (about 100 mg) was slightly off composition, containing a minor amount of $SrAl_2O_4$. However, the presence of this impurity in no way affects the data presented here.

NMR spectra were collected with Varian Unity/Inova spectrometers at 14.1 and 18.8 T fields. Aluminum-27 frequencies were 156.3 and 208.4 MHz, and spectra were referenced to external acidified 1 M $Al(NO_3)_3$ solutions in glass tubes. MAS spectra were collected with Varian/Chemagnetics "T3"-type probes, with 3.2 mm zirconia rotors spinning at 18 to 24 kHz. Single-pulse acquisitions used radio frequency (rf) tip angles of 10° (as measured for the liquid standard) with 0.2 to 0.25 μs pulses and instrumental deadtimes of about 4 μs. A triple-quantum MAS (3QMAS) spectrum for SA6 was collected at 14.1 T using a shifted-echo pulse sequence.[18] The optimized lengths of the triple quantum excitation and reconversion pulses were about 2.2 and 0.6 μs, with an rf power of 164 kHz. A soft 180° pulse, selecting the central transition only, immediately after an echo time of 1 ms, was set to 20 μs at an rf power of 11 kHz. About 200 t_1 increments with 96 FIDs per t_1 point were collected with a delay of 3 s. The 3QMAS data was processed using the "RMN" program (P. J. Grandinetti, Ohio State University), including a shear transformation.

Different strategies were chosen to extract δ_{iso}, C_Q, and η from the MAS NMR peaks, depending on the size of C_Q. The 3QMAS data provided a rough estimation of these parameters for SA6 as well. For the sites with small C_Q (Al(1) and Al(4) in Table 1), the parameters were determined from the positions of the central peak of the 1/2 to −1/2 transition and the sideband manifolds of the inner satellite transitions[19] using the Varian STARS simulation program.[20] For the sites with larger C_Q and with well-defined central-transition line shapes (Al(2) and Al-(3)), these were fitted with the same software, again optimizing results for data from both fields. The NMR parameters for the Al(5) site were relatively difficult to obtain because of its larger broadening, which is probably related to disorder (see below). The quadrupolar parameters previously reported from data obtained at 4.7 T[16] were thus chosen as constraints for our simulation of this site, as distributions of chemical shifts have less effect at lower fields and the quadrupolar line shape is more apparent.

The relative populations of Al sites were obtained from simulations of the entire group of central peaks of the 1/2 to −1/2 transitions in the MAS spectra using the program "Wsolid" (R. E. Wasylishen and K. E. Eichele, Dalhousie University, 1999) with an approximation of infinite spinning speed. δ_{iso}, C_Q, and η for each site were constrained as described above. Mixed Gaussian and Lorentzian broadenings were applied to fit the experimental line shapes. The relative intensities obtained from the simulations were then corrected for the differences in the populations of the central and satellite transitions in the central peaks (I_{iso} factors in Table 1), which depend on the quadrupolar parameters and experimental conditions such as Larmor frequency, radio frequency power and spinning rate.[21] The peak areas at 14.1 T were derived from the relative areas obtained from fits at 18.8 T by taking into account the values of I_{iso} at the two fields and were used in the simulations shown in the figures.

TABLE 1: Al-27 NMR Parameters for CA6 and SA6[a]

				18.8 T		14.1 T		corr.	ideal
site	δ_{iso} (ppm)	C_Q (MHz)	η	area (%)	I_{iso}[b] ± 0.04	area (%)	I_{iso}[b] ± 0.04	area[c] (%)	area[c] (%)
SA6:									
Al(1)	16.72(5)	0.25(5)	n.d.	17.2(5)	2.36	17.2	2.33	8.2	8.3
Al(2)	57.8(1)	20.75(5)	0.00(5)	4.9(2)	0.67	3.6	0.48	8.2	8.3
Al(3)	67.5(1)	3.45(5)	0.00(5)	14.8(5)	1.05	15.1	1.05	16.0	16.7
Al(4)	9.45(5)	1.35(5)	n.d.	16.7(5)	1.13	16.9	1.13	16.6	16.7
Al(5)	22.1(1)	4.9(1)	0.65(10)	46.4(5)	1.03	47.2	1.03	51.0	50.0
CA6:									
Al(1)	16.26(5)	0.15(5)	n.d.	20.3(5)	2.77	23.3	3.29	8.3	8.3
Al(2)	55.8(1)	21.40(5)	0.00(5)	4.5(2)	0.63	3.2	0.46	8.2	8.3
Al(3)	68.1(1)	3.10(5)	0.00(5)	14.4(5)	1.00	14.5	1.04	16.4	16.7
Al(4)	9.92(5)	1.60(5)	n.d.	15.8(5)	1.10	15.1	1.09	16.3	16.7
Al(5)	22.3(5)	4.8(1)	0.7(1)	45.0(5)	1.01	43.9	1.02	50.8	50.0

[a] Values of η for the sites with the lowest C_Q values could not be determined. [b] I_{iso} is the calculated intensity correction factor that depends on quadrupolar parameters and experimental conditions.[21] [c] Corrected relative peak area from fits and I_{iso} at 18.8 T; ideal area from X-ray structure.

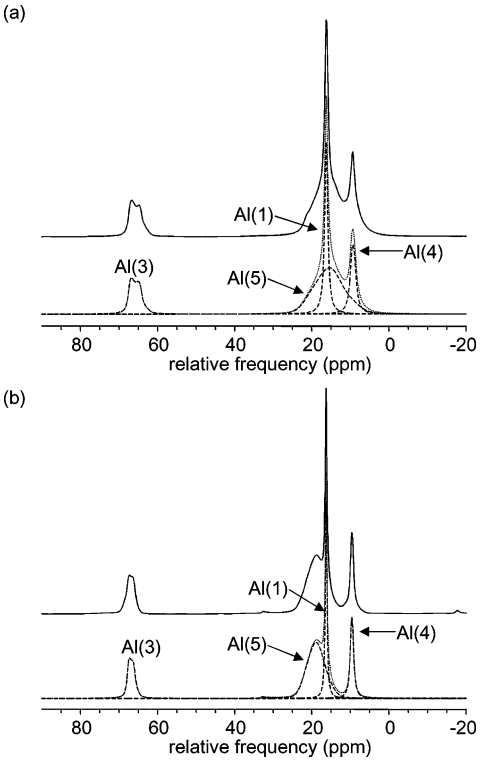

Figure 1. Aluminum-27 MAS spectra of CA6 at (a) 14.1 T and spinning rate of 23 kHz and (b) 18.8 T and 18 kHz. Fitted components and their sum are shown by dashed and dotted lines, respectively, as described in text and Table 1.

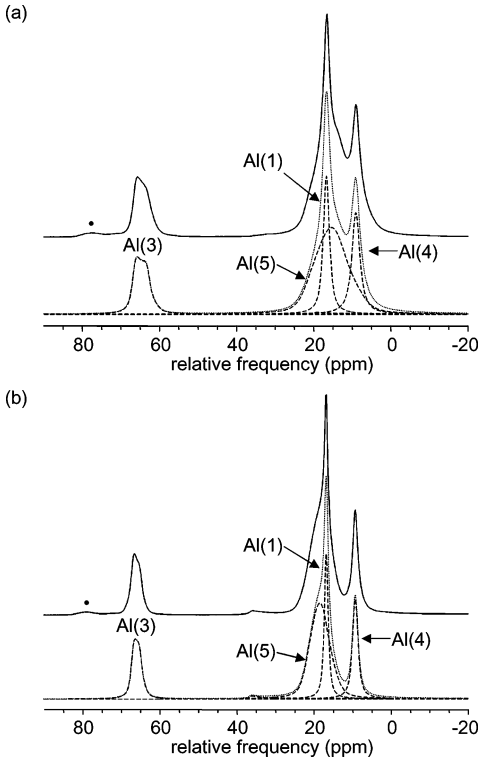

Figure 2. Aluminum-27 MAS spectra of SA6 at (a) 14.1 T and spinning rate of 23 kHz and (b) 18.8 T and 24 kHz. Fitted components and their sum are shown by dashed and dotted lines, respectively, as described in text and Table 1. Filled circle marks a peak from a small amount of $SrAl_2O_4$.

Results and Discussion

Experimental and simulated ^{27}Al MAS for CA6 and SA6 are shown in Figures 1, 2, and 3. Those at 14.1 T are quite similar to previously published data,[13,14,16,17] and are similar to each other, as expected for isostructural compounds. The higher frequency peak (about 65 ppm) can be fitted with a single quadrupolar doublet (Table 1), consistent with the single "normal" tetrahedral site in the structures (Al(3), following previous nomenclature[4,5]). The region between about 20 and 0 ppm contains two narrow peaks, which, again as previous authors have found, are consistent with the relatively symmetrical octahedral Al(1) and Al(4) sites.[16,17] This region of the spectrum also contains a broader peak with no well-defined quadrupolar line shape; previous authors have fitted this with two components representing the less symmetrical Al(5) octahedron, plus the "pentahedral" Al(2) site.[16,17]

In the 18.8 T spectra, however, careful examination of the baseline, and adjustment of the sample spinning rate to optimize sideband positions, revealed a previously unreported component for both SA6 and CA6, which can be accurately fitted with C_Q values of about 21 MHz, $\eta = 0$, and δ_{iso} of about 57 ppm, with relative areas of close to the 8.3% expected for the Al(2) site (Figure 3, Table 1). This new component was observed in at least two samples of each phase; it is most apparent at 18.8 T, but its lower frequency singularity can readily be identified at 14.1 T as well. We interpret this doublet as resulting from Al(2) atoms in highly distorted tetrahedra, displaced from the ideal central position of the "trigonal bipyramid" site and thus fully consistent with the static version of the split-atom model. (The NMR data, of course, do not preclude intrasite hopping at a frequency slow compared to the time scale of the measurement, which is roughly defined here by the ≈15 kHz peak width.)

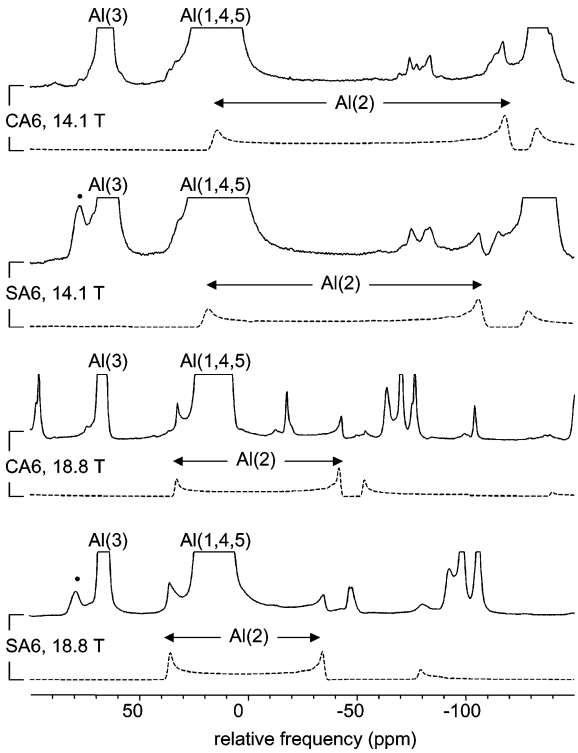

Figure 3. Aluminum-27 MAS spectra of CA6 and SA6, with expanded scales to show Al(2) with very large C_Q values. Dashed line shows simulation for Al(2) only, arrows mark central transition. Central peaks for other Al sites are labeled; solid dot marks $SrAl_2O_4$ impurity; other features are spinning sidebands.

The remaining broad peak in the 30 to 0 ppm region must thus be mainly due to the distorted octahedral site Al(5). Its poorly defined line shape is likely to be the result of the disorder in the Al(2) positions as observed in the split-atom refinements:[16] two Al(5) atoms are bonded to each of the equatorial oxygens (O(3)) of the Al(2) site, and thus their disorder could have a particularly large effect on the latter. Our assignments of the three octahedral peaks are consistent with their relative degrees of distortion from ideal octahedral symmetry as proposed from early single-crystal NMR[22] and as tested for SA6 MAS NMR data;[16] fitted peak areas for all five Al sites agree remarkably well with those expected from the X-ray structures (Table 1), and thus the calculated spectra agree very well with the experimental data at both fields.

In Figure 4 we show the 3QMAS ^{27}Al spectrum for SA6, collected at 14.1 T, for comparison with previous work.[16] Only three peaks are visible, corresponding to Al(3), Al(4), and Al-(5), in positions consistent with the MAS data. The signals from the other two sites are not readily detectable because of the very low efficiency of multiple quantum excitation and reconversion caused by their extremely small (Al(1)) and extremely large (Al(2)) C_Q values.

The quadrupolar asymmetry parameter for the Al(2) site is not measurably different from 0, which is the value expected for an atom on a crystallographic 3-fold axis; the same is true for the symmetrical Al(3) tetrahedron. The C_Q values for the Al(2) sites of about 21 MHz are probably the largest reported for Al coordinated by O in any material and must be related to the unusual distortions of these sites. The latter is obvious in the contrast between the apical Al−O distance and the three equatorial distances, which for split-atom structures of SA6 are 0.2025 vs 0.1765 nm [4] and for CA6 are 0.2040 vs 0.1751.[5] The relationship of this distortion to C_Q can be explored in a simple fashion by calculating a "longitudinal strain" index[22] from the

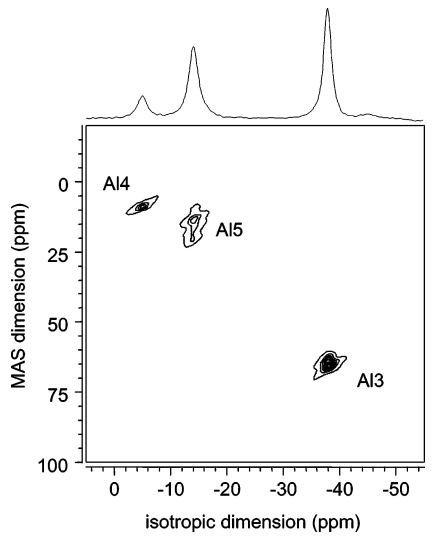

Figure 4. Aluminum-27 3QMAS spectrum of SA6, plotted with axes and scales as described previously.[29]

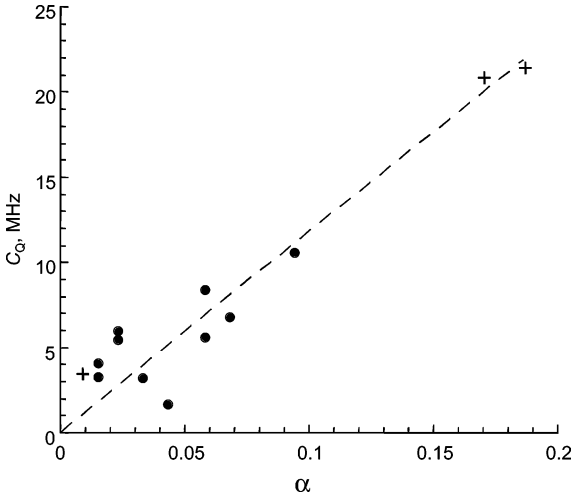

Figure 5. Plot of C_Q vs "longitudinal strain index" α for tetrahedral Al sites in oxides. Solid circles show single-crystal data as described in an early description of such correlations;[22] crosses show data for Al(2) sites in SA6 and CA6 and Al(3) site in SA6.

ratios of the observed Al−O bond distances (l_i) to those of a fully symmetrical tetrahedron of identical volume (l_0):

$$\alpha = \sum |\ln(l_i/l_0)| \qquad (1)$$

In Figure 5 are plotted the results from the single-crystal data reported in the original discussion of this correlation, together with the new results for CA6 and SA6. Although the correlation is rough (as expected from its reliance on simple first-neighbor geometry alone), the very high C_Q values for the Al(2) sites do seem to be sensible, as do the low values for the Al(3) sites.

The δ_{iso} values for the distorted tetrahedra are at the low end of the range of known values for Al with four oxygen neighbors, especially for such sites in aluminates, which are typically between 70 and 86 ppm for phases such as $CaAl_2O_4$ ("CA") and $CaAl_4O_7$ ("CA2").[23,24] It is likely that the large average Al−O bond distances for the split-atom models of these sites (0.1830 and 0.1823 nm for Al(2) in SA6 and CA6, vs 0.1802 nm for Al(3) in SA6, and ≈0.175 nm in CA and CA2[25,26]) contribute to these extreme values. For the Al(2) sites also, the much longer distances to the distant apical oxygen of the trigonal pyramidal site (0.245 nm in SA6, 0.238 nm in CA6) are apparently too great to assert much influence on δ_{iso}.

Finally, we note that, with the exceptions of phosphates, δ_{iso} for Al in truly "well-defined" pentacoordinate sites in oxides now all seem to fall in the range from about 30 to 52 ppm.[16,27] It is thus likely that the speculation that a peak at 15 ppm in the ^{27}Al spectrum of Al-containing $MgSiO_3$ perovskite might be distorted AlO_5 sites[28] is not a correct assignment.

Acknowledgment. This work was supported by NSF grant EAR 0104926. We thank J. Puglisi and C. Liu for access to, and assistance with, the 18.8 T spectrometer in the Stanford Magnetic Resonance Laboratory.

References and Notes

(1) Collongues, R.; Gourier, D.; Kahn-Harari, A.; Lejus, A. M.; Théry, J.; Vivien, D. *Annu. Rev. Mater. Sci.* **1990**, *20*, 51−82.
(2) Lindop, A. J.; Matthews, C.; Goodwin, D. W. *Acta Crystallogr.* **1975**, *B31*, 2940−2941.
(3) Kato, K.; Saalfeld, H. *N. Jahrb. Mineral. Abh.* **1968**, *109*, 192−200.
(4) Kimura, K.; Ohgaki, M.; Tanaka, K.; Morikawa, H.; Marumo, F. *J. Solid State Chem.* **1990**, *87*, 186−194.
(5) Utsunomiya, A.; Tanaka, K.; Morikawa, H.; Marumo, F.; Kojima, H. *J. Solid State Chem.* **1988**, *75*, 197−200.
(6) Bermanec, V.; Holtsam, D.; Sturman, D.; Criddle, A. J.; Back, M. E.; Scavnicar, S. *Can. Mineral.* **1996**, *34*, 1287−1297.
(7) An, L.; Ha, H.-C.; Chan, H. M. *J. Am. Ceram. Soc.* **1998**, *81*, 3321−3324.
(8) Engelhardt, G.; Michel, D. *High-Resolution Solid-State NMR of Silicates and Zeolites*; Wiley: New York, 1987.
(9) Stebbins, J. F. Nuclear magnetic resonance spectroscopy of silicates and oxides in geochemistry and geophysics. In *Handbook of Physical Constants*; Ahrens, T. J., Ed.; American Geophysical Union: Washington D. C., 1995; Vol. 2, pp 303−332.
(10) Bunker, B. C.; Kirkpatrick, R. J.; Brow, R. K.; Turner, G. L.; Nelson, C. *J. Am. Ceram. Soc.* **1991**, *74*, 1430−1438.
(11) Yarger, J. L.; Smith, K. H.; Nieman, R. A.; Diefenbacher, J.; Wolf, G. H.; Poe, B. T.; McMillan, P. F. *Science* **1995**, *270*, 1964−1967.
(12) Stebbins, J. F.; Kroeker, S.; Lee, S. K.; Kiczenski, T. J. *J. Non-Cryst. Solids* **2000**, *275*, 1−6.
(13) Müller, D.; Gessner, W.; Samoson, A.; Lippmaa, E. *Polyhedron* **1986**, *5*, 779−785.
(14) van Hoek, J. A. M.; van Loo, F. J. J.; Metselaar, R.; de Haan, J. W. *Solid State Ionics* **1991**, *45*, 93−100.
(15) Veeman, W. S. *Z. Naturforsch.* **1992**, *47a*, 353−360.
(16) Jansen, S. R.; Hintzen, H. T.; Metselaar, R.; de Haan, J. W.; van de Ven, L. J. M.; Kentgens, A. P. M.; Nachtegaal, G. H. *J. Phys. Chem. B* **1998**, *102*, 5969−5976.
(17) Gervais, C.; MacKenzie, K. J. D.; Smith, M. E. *Magn. Res. Chem.* **2001**, *39*, 23−28.
(18) Massiot, D.; Touzo, B.; Trumeau, D.; Coutures, J. P.; Virlet, J.; Florian, P.; Grandinetti, P. J. *Solid State NMR* **1996**, *6*, 73−83.
(19) Jäger, C.; Müller-Warmuth, W.; Mundus, C.; van Wüllen, L. *J. Non-Cryst. Solids* **1992**, *149*, 209−217.
(20) Skibsted, J.; Nielsen, N. C.; Bildsøe, H.; Jakobsen, H. J. *J. Magn. Reson.* **1991**, *95*, 88−117.
(21) Massiot, D.; Bessada, C.; Coutures, J. P.; Taulelle, F. *J. Magn. Reson.* **1990**, *90*, 231−242.
(22) Ghose, S.; Tsang, T. *Am. Mineral.* **1973**, *58*, 748−755.
(23) Skibsted, J.; Henderson, E.; Jakobsen, H. J. *Inorg. Chem.* **1993**, *32*, 1013−1027.
(24) Stebbins, J. F.; Oglesby, J. V.; Kroeker, S. *Am. Mineral.* **2001**, *86*, 1307−1311.
(25) Goodwin, D. W.; Lindop, A. J. *Acta Crystallogr.* **1970**, *B26*, 1230−1235.
(26) Hörkner, W.; Müller-Buschbaum, H. K. *J. Inorg. Nucl. Chem.* **1976**, *38*, 983−984.
(27) Fyfe, C. A.; Bretherton, J. L.; Lam, L. Y. *Chem. Commun.* **2000**, *2000*, 1575−1576.
(28) Stebbins, J. F.; Kojitani, H.; Akaogi, M.; Navrotsky, A. *Am. Mineral.* **2003**, *88*, 1161−1164.
(29) Baltisberger, J. H.; Xu, Z.; Stebbins, J. F.; Wang, S.; Pines, A. *J. Am. Chem. Soc.* **1996**, *118*, 7209−7214.